Electronic Supplementary Material (ESI) for Physical Chemistry Chemical Physics.

Binding of synthetic nanobodies to SARS-CoV-2 receptor-binding domain: the importance of salt bridge

Hujun Shen,* Hengxiu Yang

Guizhou Provincial Key Laboratory of Computational Nano-Material Science, Guizhou Education University, Guiyang 550018, China.

Supporting Information

*Corresponding author email: hujun.shen@hotmail.com

Table S1. The hydrogen bonds and salt bridges formed between ACE2 and SARS-CoV-2 RBD, obtained from the X-ray crystal structure of RBD-ACE2 complex.

	RBD	ACE2
Hydrogen bonds	LYS417(NZ)	ASP30(OD1)
	TYR449(OH)	ASP38(OD1/OD2)
	TYR449(OH)	GLN42(NE2/OE1)
	ASN487(ND2)	GLN24(OE1)
	ASN487(OD1)	TYR83(OH)
	TYR489(OH)	GLN42(NE1/NE2)
	TYR489(OH)	TYR83(OH)
	GLN493(NE2)	GLU35(OE2)
	THR500(OG1)	TYR41(OH)
	ASN501(N)	TYR41(OH)
	TYR505(OH)	GLU37(OE2/OE1)
Salt bridges	LYS417(N)	ASP30(OD1)
	LYS417(N)	ASP30(OD2)

Figure S1. The RMSD curve for the backbone heavy atoms of RBD, obtained from

microsecond MD simulation of the RBD model in the ligand-free form (RBD).

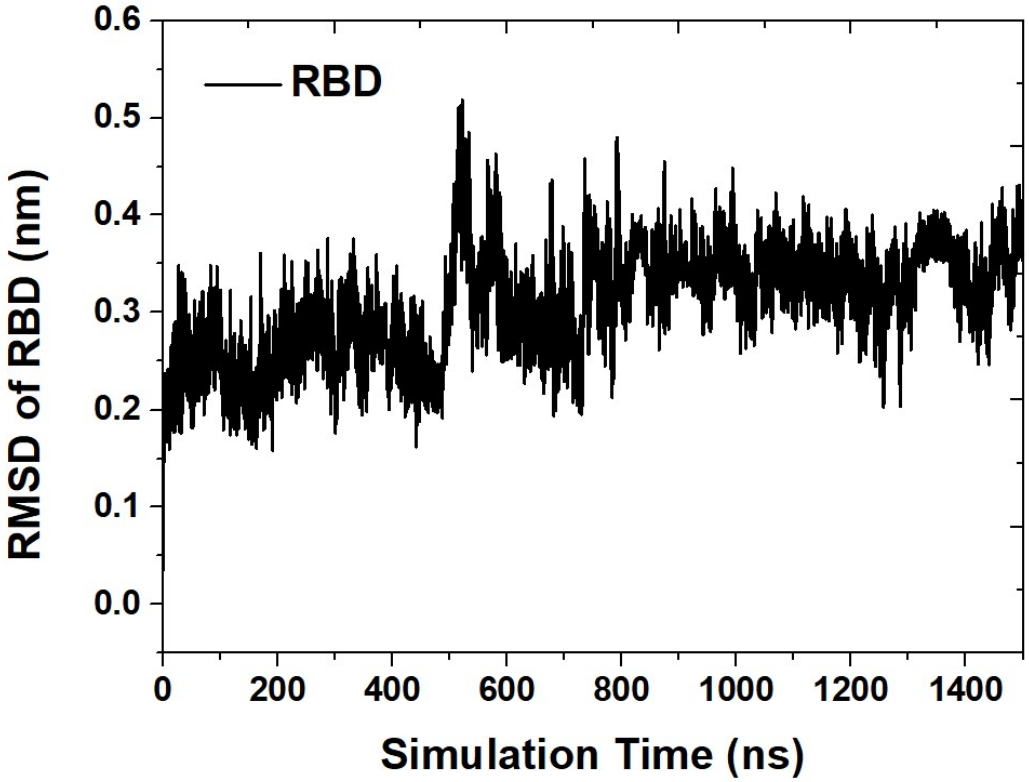

Figure S2. The RMSD curve for the backbone heavy atoms of RBD, obtained from

microsecond MD simulation of the RBD model in the Sb16-bound form (Sb16-RBD):(A) five independent simulations and (B) one simulation was extended to 1000 ns

(A)

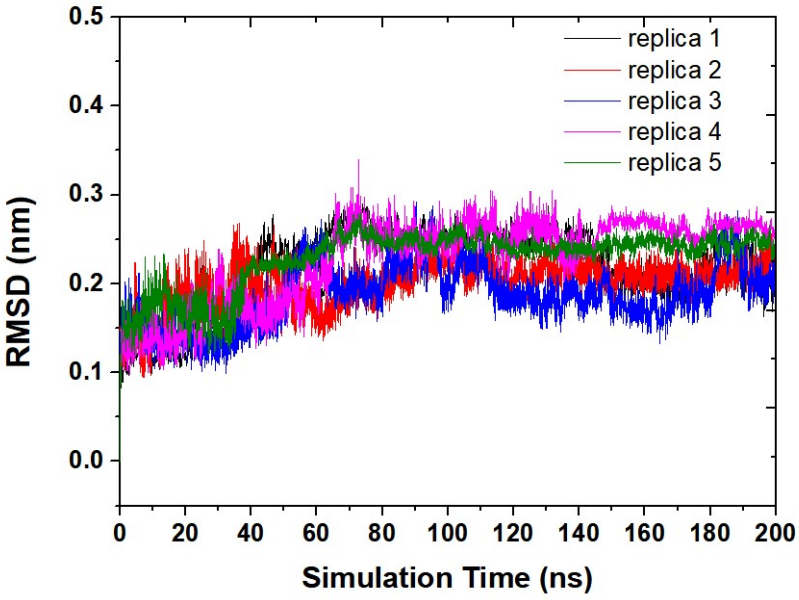

(B)

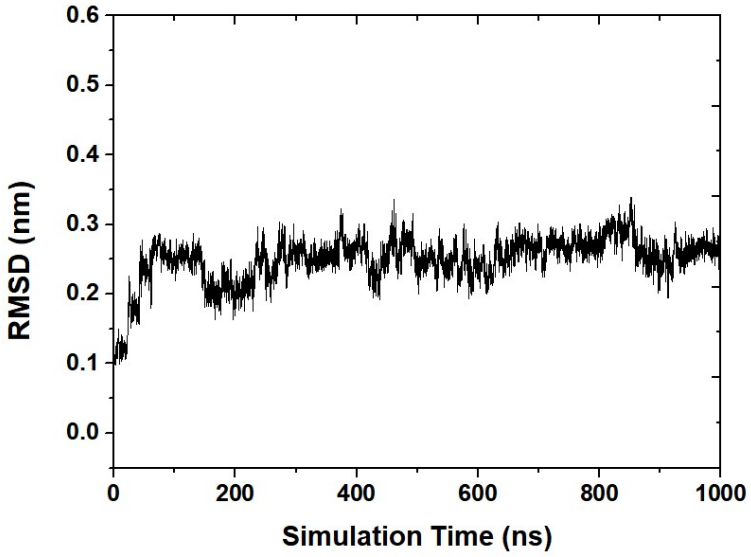

Figure S3. The RMSD curve for the backbone heavy atoms of RBD, obtained from

microsecond MD simulation of the RBD model in the Sb45-bound form (Sb45-RBD): (A) five independent simulations and (B) one simulation was extended to 1000 ns.

(A)

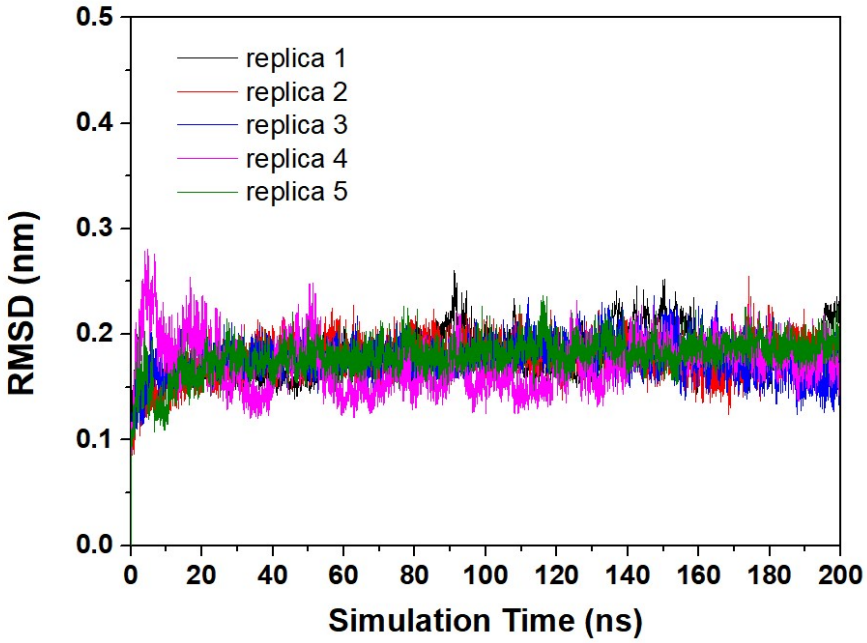

(B)

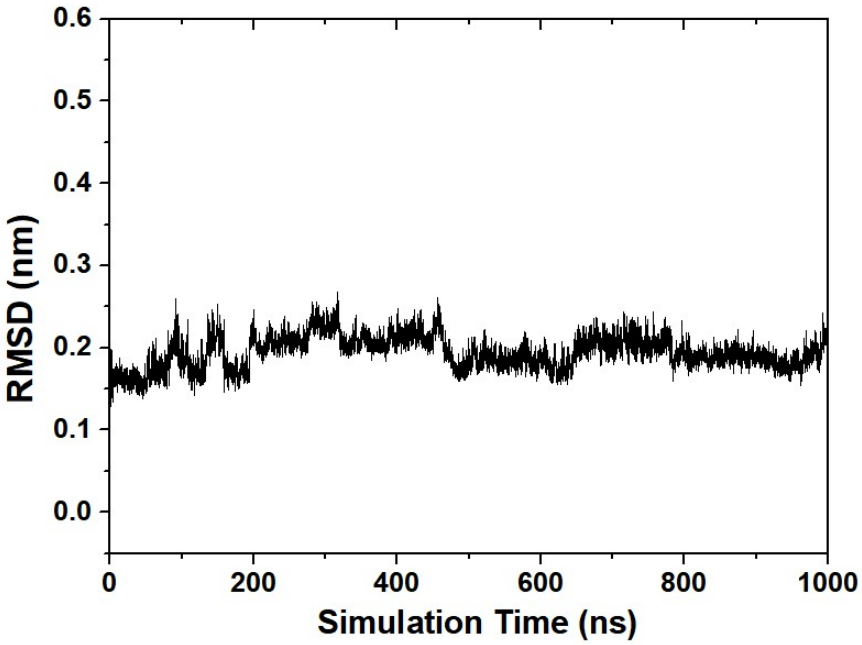

Figure S4. The RMSD curve for the backbone heavy atoms of RBD, obtained from

microsecond MD simulation of the RBD mutant K417N in the Sb16-bound form (K417N): (A) five independent simulations and (B) one simulation was extended to 1000 ns

(A)

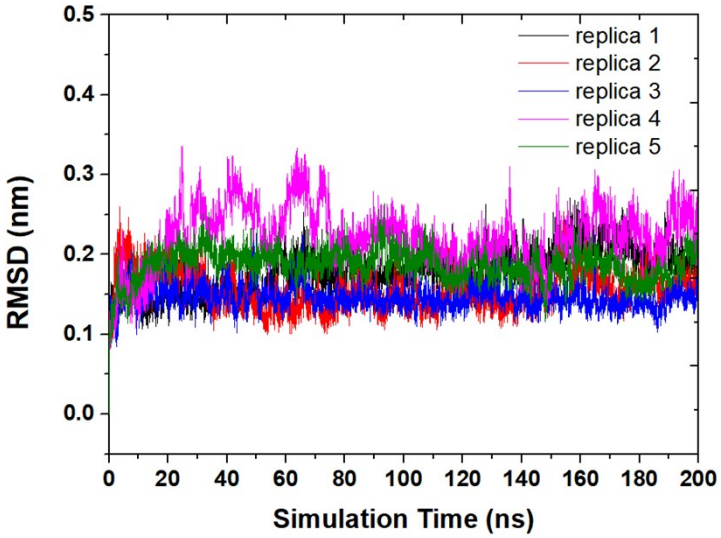

(B)

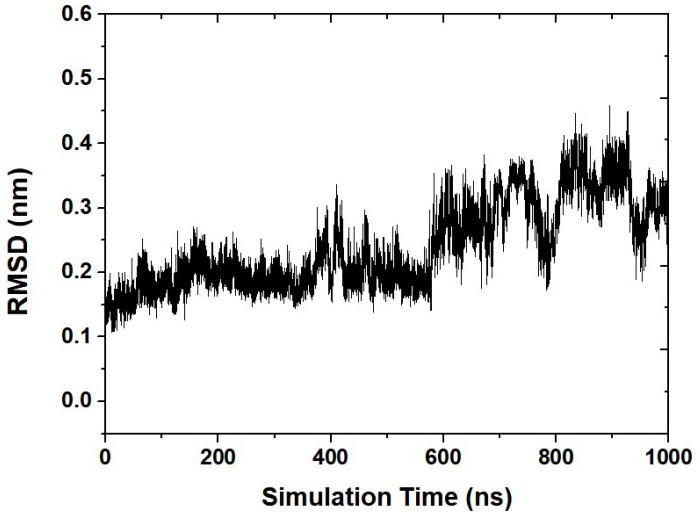

Figure S5. The RMSD curve for the backbone heavy atoms of RBD, obtained from microsecond MD simulation of the RBD mutant E484K in the Sb16-bound form (E484K): (A) five independent simulations and (B) one MD simulation was extended to 1000 ns

(A)

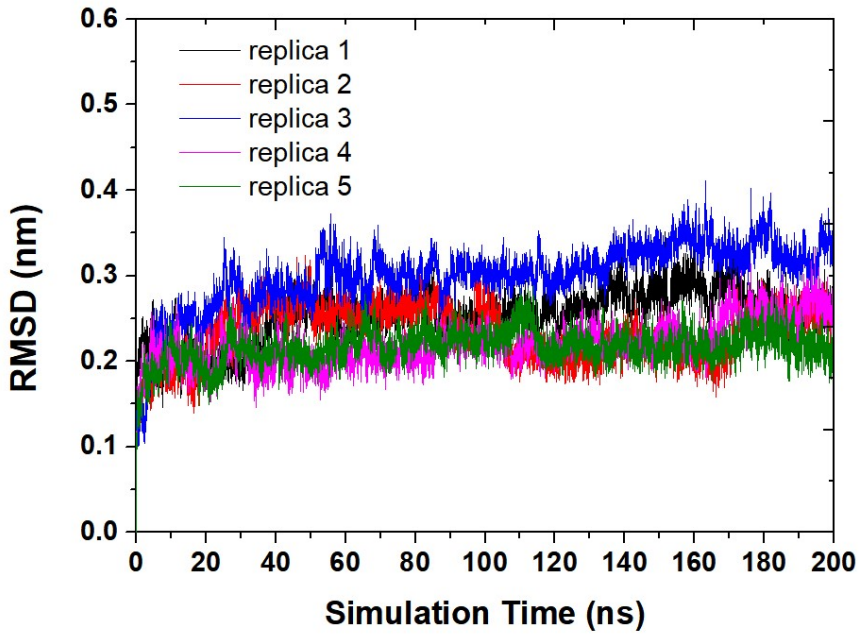

(B)

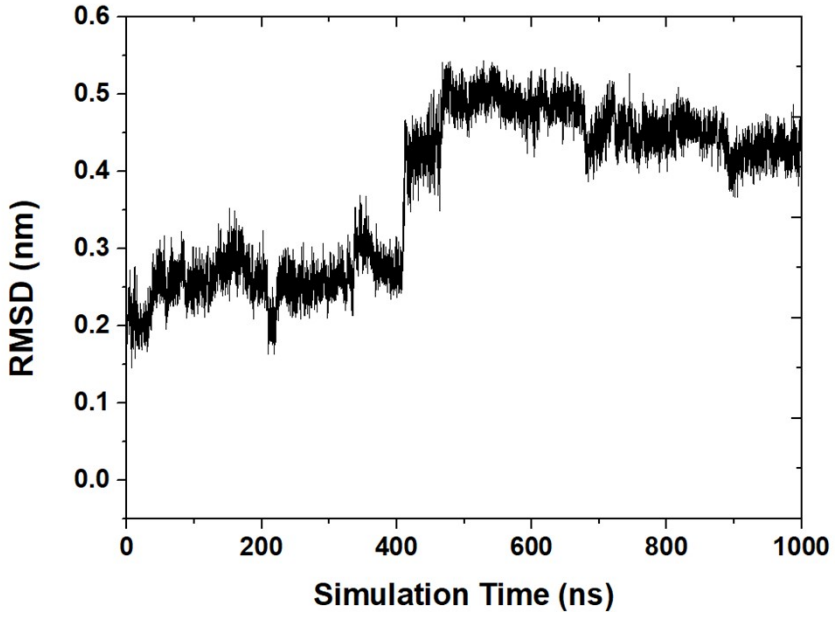

Figure S6. Alignment of the average structures of RBD in the ligand-free form

obtained from two different simulation windows: t_1=200-400 ns (green) and t_2=500-700 ns (red). The two RBD loop regions (ASP442-TYR453, GLU471-SER494) are labeled with RBD loop I and RBD loop II respectively.

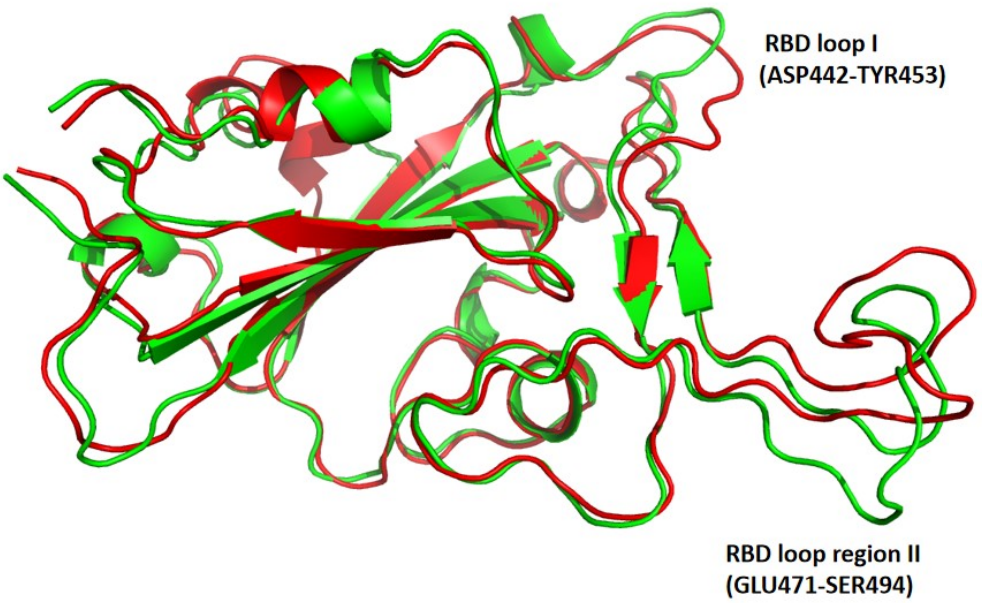

Figure S7. Alignment of the average structures of RBD in the (A) Sb16-bound form

and (B) Sb45-bound form obtained from two different simulation windows: t_1=200-400 ns (green) and t_2=500-700 ns (red). The two RBD loop regions (ASP442-TYR453, GLU471-SER494) are labeled with RBD loop I and RBD loop II respectively.

(A)

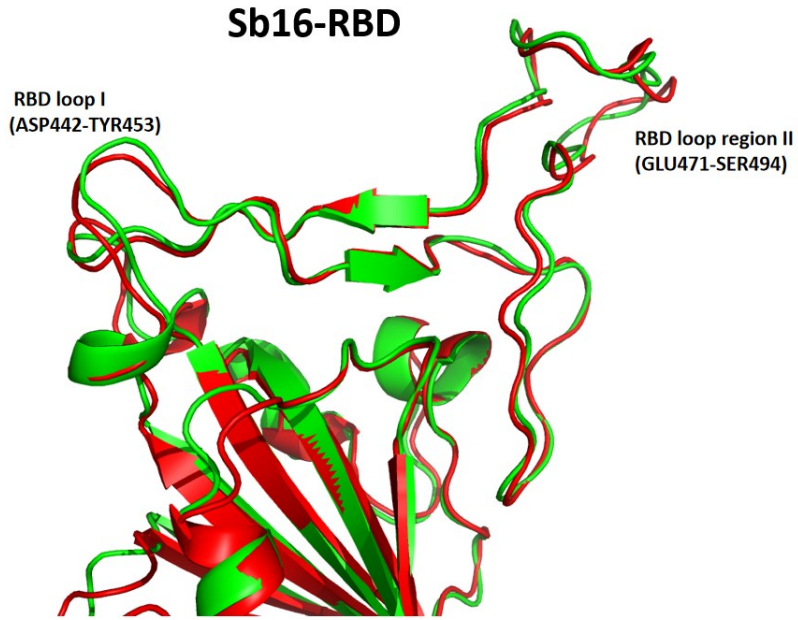

(B)

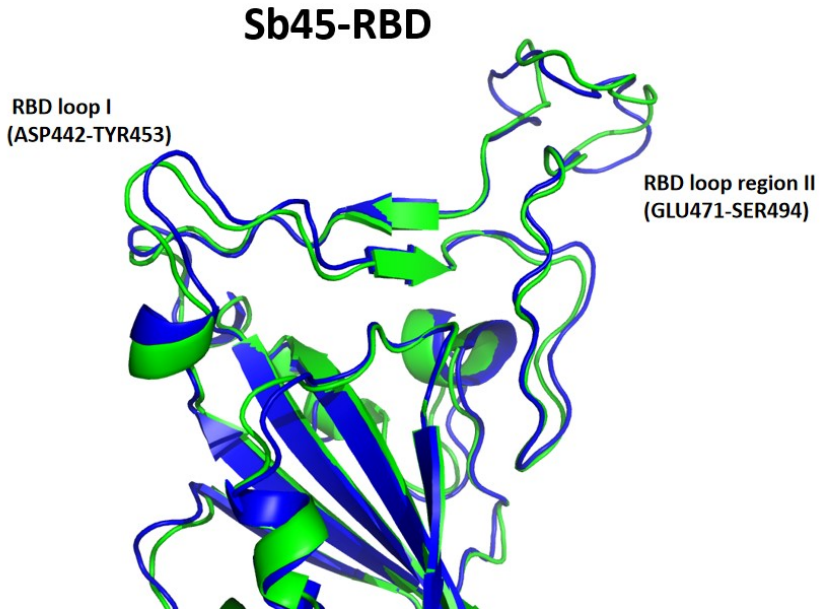

Figure S8. The probability distribution for the distances between the atom CD of GLU484 in RBD and the atom CZ of ARG33 in Sb45, constructed from the 1.0-μs MD simulations of the Sb45-RBD complexes.

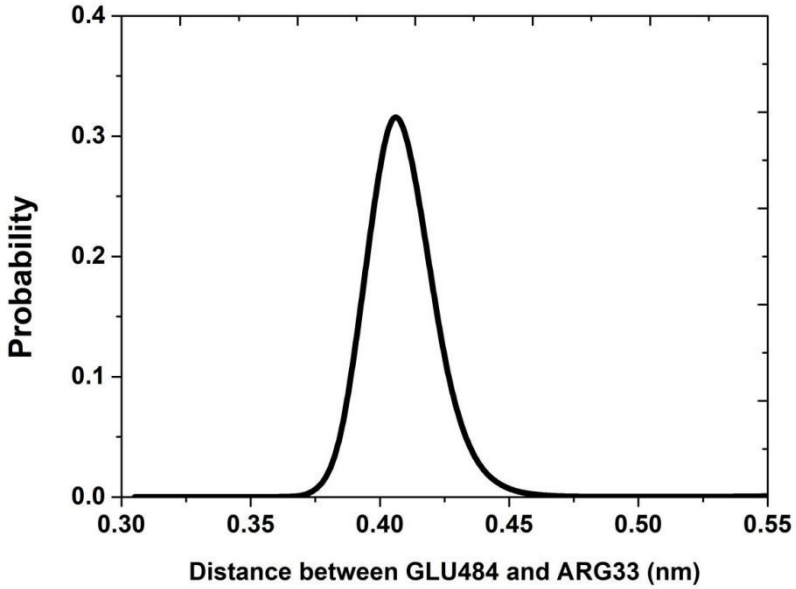

Figure S9. The probability histogram plots for (A) PC1 and (B) PC2 obtained from the MD simulation of the Sb16-RBD binding model.

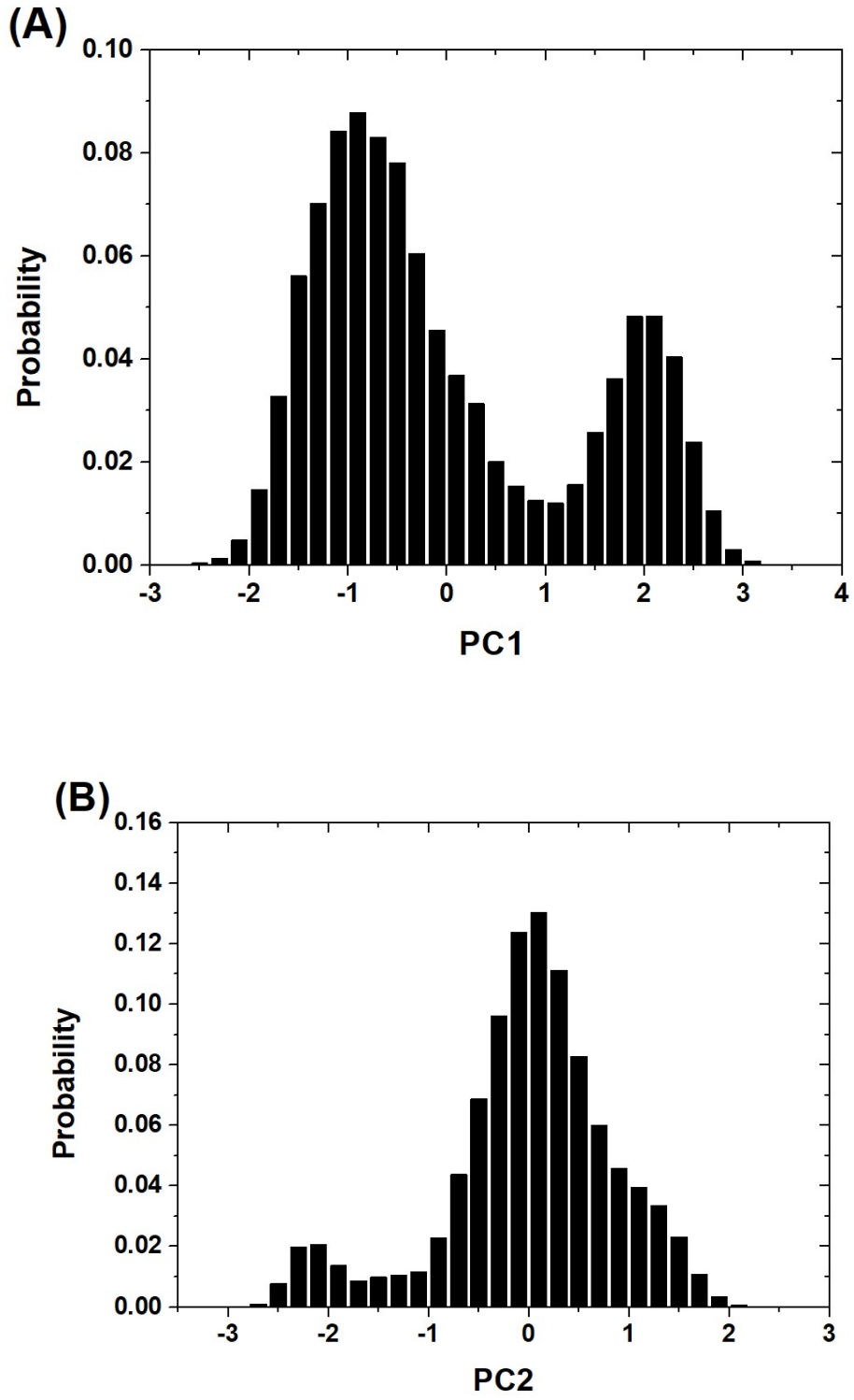

Figure S10. The probability histogram plots for (A) PC1 and (B) PC2, obtained from the MD simulation of the Sb45-RBD binding model.

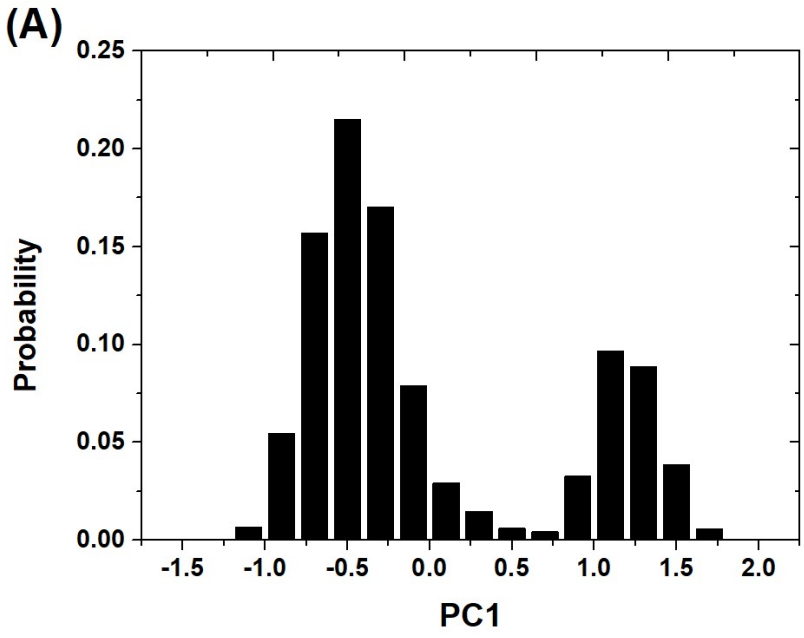

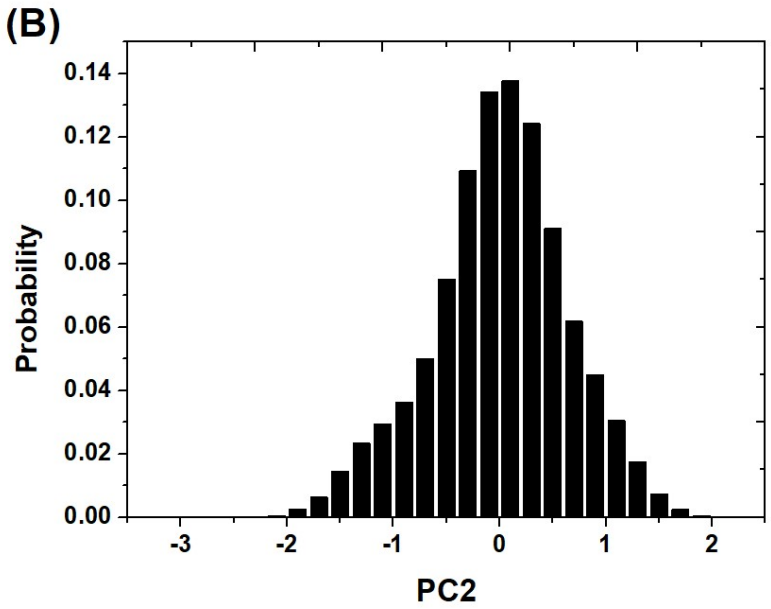

Figure S11. Cartoon representation of three binding modes in Sb16-RBD complex obtained from microsecond MD simulation. The four residues LYS32, THR33, GLU484, and GLN493 are represented by sticks. The flexible RBD loop and the CDR1 region Sb16 are indicated in green and red.

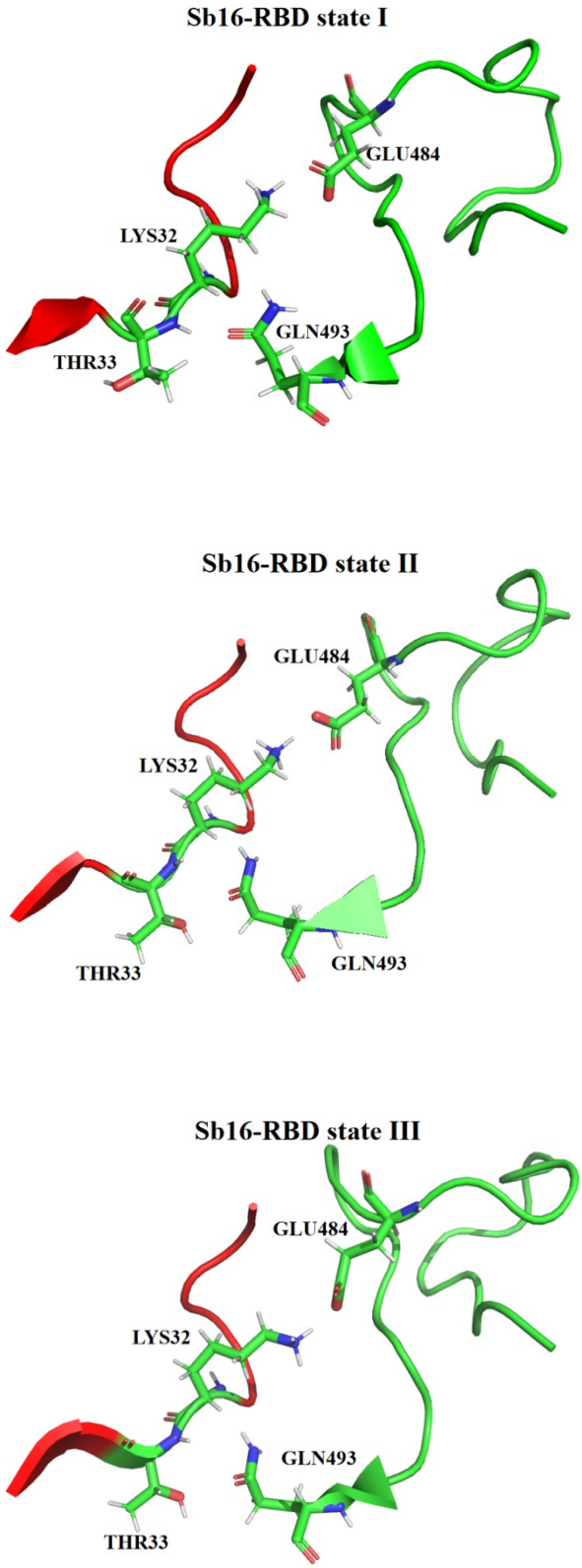

Figure S12. Cartoon representation of two binding modes in Sb45-RBD complex obtained from microsecond MD simulation. The four residues ASP32, ARG33, GLU484, and SER494 are represented by sticks. The flexible RBD loop and the CDR1 region Sb45 are indicated in green and blue.

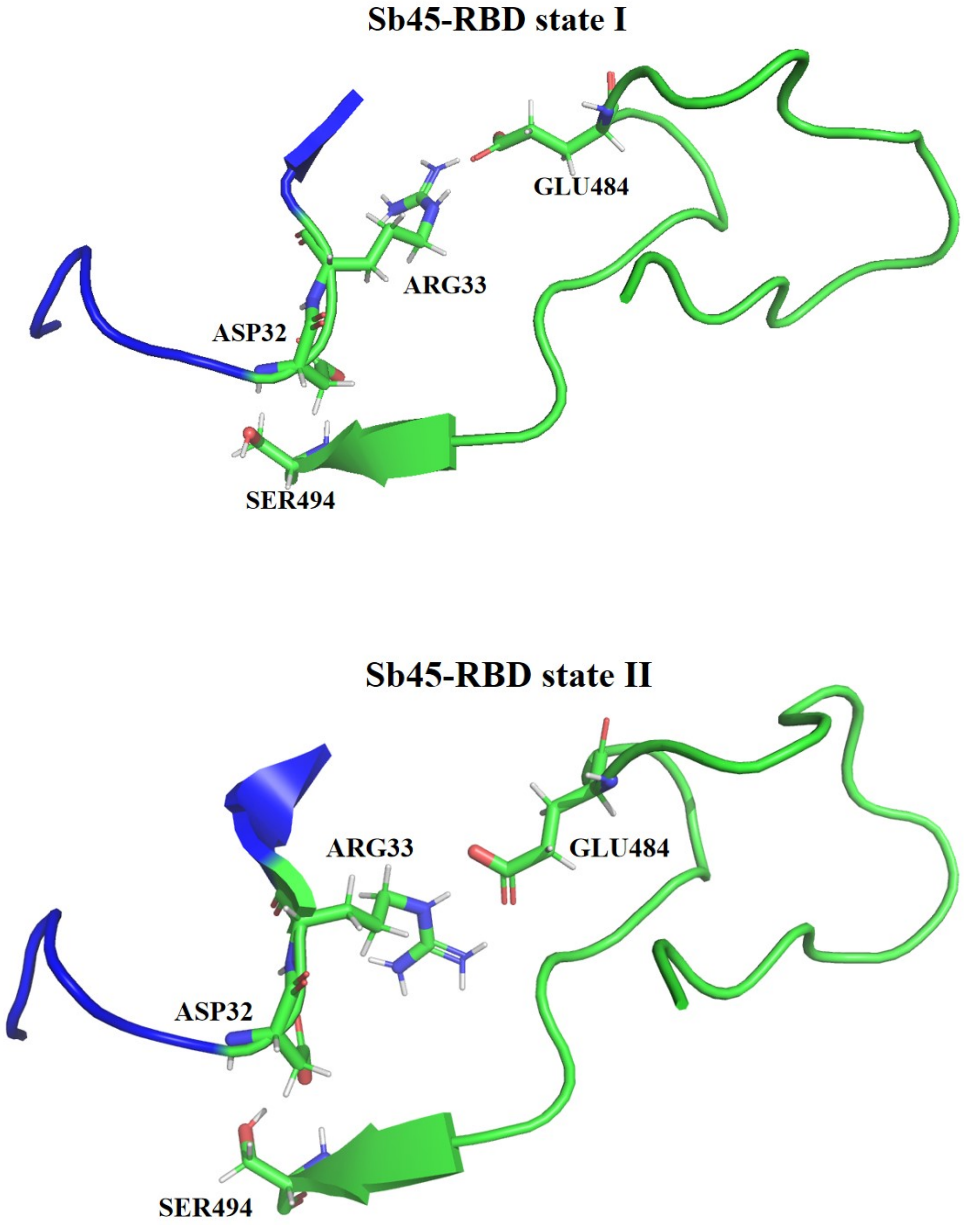

Figure S13. Residue-wise energy contribution spectra and the comparison between (A) Sb16-RBD and (B) SB45-RBD with the largest binding affinity. Amino acid residues are only displayed when the residue pairs between RBD and nanobodies are within a distance of 4.0 Å. The residues with an energy contribution below -4 kcal/mol are indicated with blue color, those between -4 and -2 kcal/mol with green color, and those between 0 and -2 kcal/mol with red color. Three CDR regions (CDR1, CDR2, and CDR3) of nanobodies and two RBD loop regions (RBD loop I and loop II) are labeled in each figure, respectively.

(A)

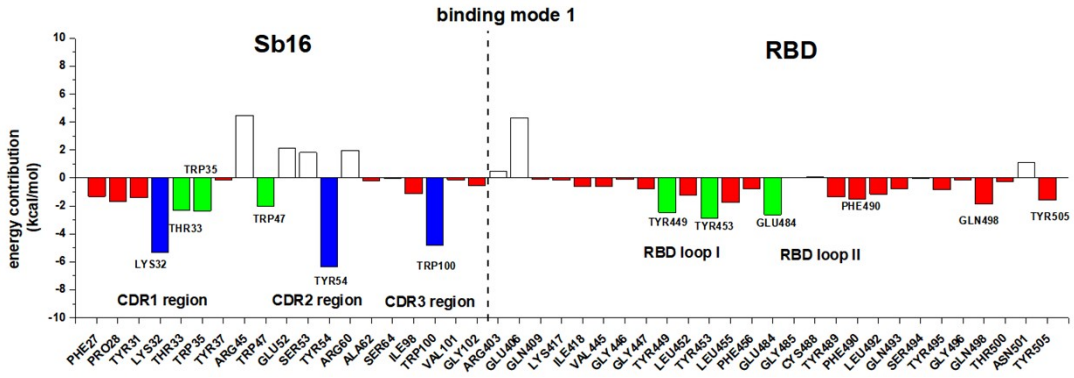

(B)

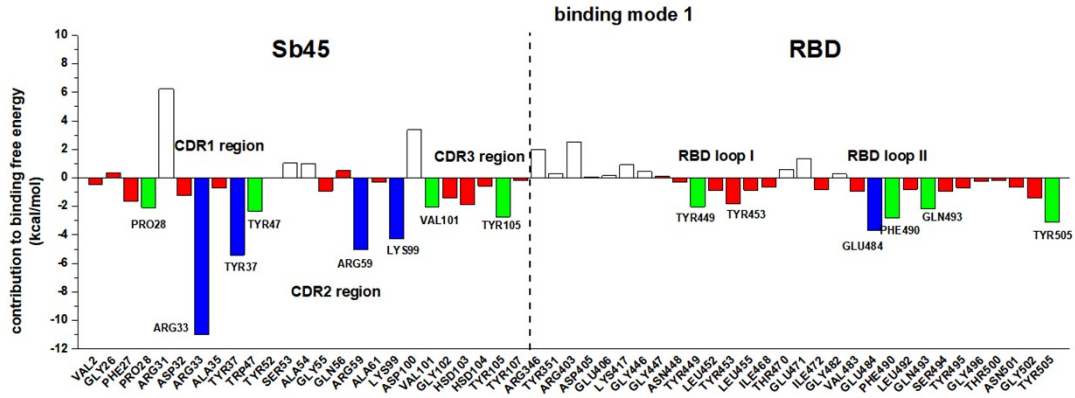

Figure S14. Alignment of the average structures of RBD in two different simulation windows: t_1=300-400 ns (green) and t_2=500-700 ns (red), obtained from MD simulations of (A) K417K and (B) E484K binding complexes with Sb16. The two RBD loop regions (ASP442-TYR453, GLU471-SER494) are labeled with RBD loop I and RBD loop II respectively.

(A)

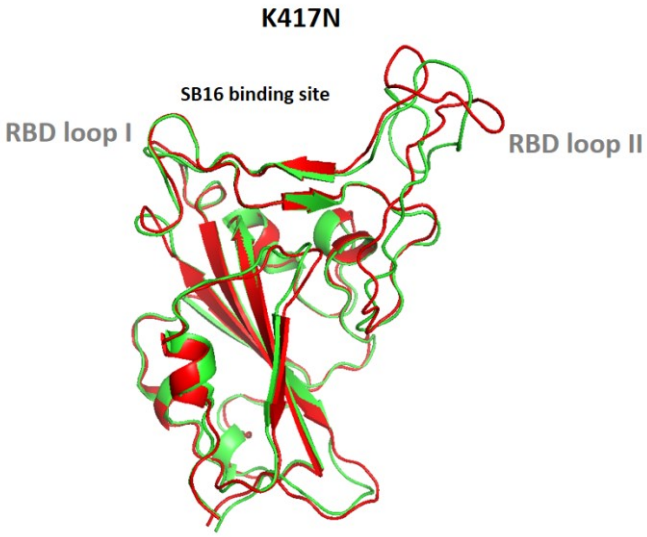

(B)

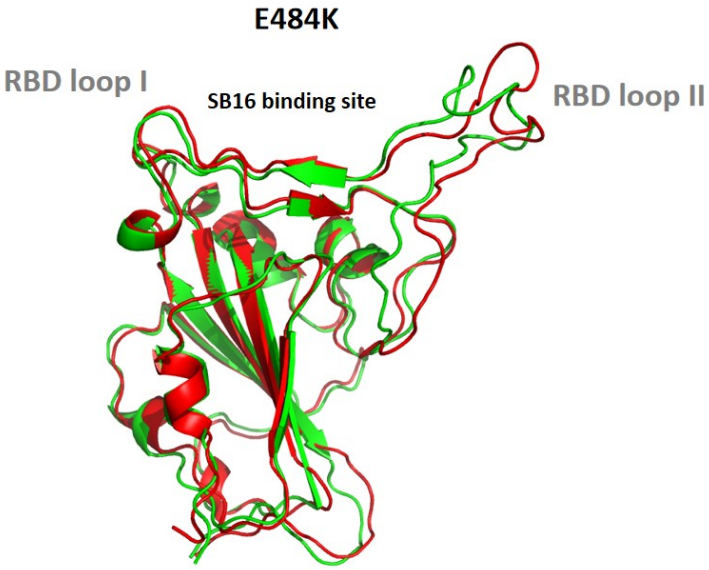

Figure S15. The probability histogram plots for (A) PC1 and (B) PC2, obtained from the MD simulation of the E484K complex model with Sb16 binding.

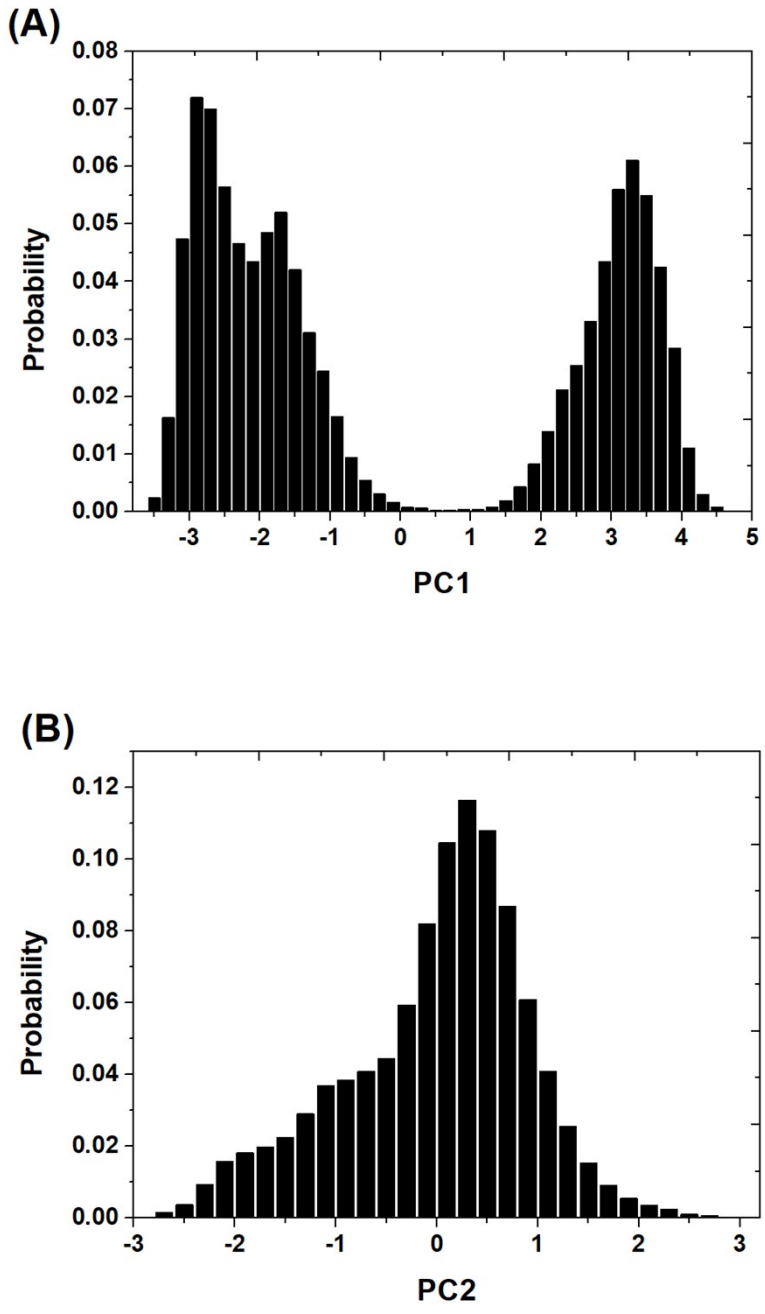

Figure S16. The probability histogram plots for (A) PC1 and (B) PC2, obtained from the MD simulation of the K417N complex model with Sb16 binding.